Applied Radiation and Isotopes 214 (2024) 111516

Contents lists available at ScienceDirect

Applied Radiation and Isotopes

journal homepage: www.elsevier.com/locate/apradiso

A custom-made integrated system for thermoluminescence and radioluminescence spectroscopy

Matheus C.S. Nunes [a,b], Miguel L. Rodrigues [c], Walace J.R. Silva [b], Ronaldo S. Silva [d], Nancy K. Umisedo [a], Elisabeth M. Yoshimura [a], Neilo M. Trindade [a,*]

[a] Instituto de Física, Universidade de São Paulo (USP), São Paulo SP, Brazil
[b] Instituto de Ciência e Tecnologia, Universidade Estadual Paulista (UNESP), Sorocaba, SP, Brazil
[c] Serviço Nacional de Aprendizagem Industrial (SENAI), Diadema, SP, Brazil
[d] Departamento de Física, Universidade Federal de Sergipe (UFS), Aracaju, SE, Brazil

ARTICLE INFO

Keywords:
Thermoluminescence
Radioluminescence
Dosimetry
Spectroscopy TL
Scientific instrumentation

ABSTRACT

Thermoluminescence (TL) and Radioluminescence (RL) are widely used in dosimetry applications. We present a custom-built integrated system, designated LUMI22, for measuring TL, TL spectroscopy, RL, and RL as a function of temperature. LUMI22 includes a heating system based on Kanthal® A1 alloy (FeCrAl), a microcontroller to regulate the temperature ramps (e.g. 1–5 °C/s). To irradiate samples an X-ray tube (Moxtek 50 kV, 50 μA) is powered, controlled, and monitored by an FTC-200 standard controller. The dose rate at the sample position is 0.43 Gy/min. Light collection includes a Photomultiplier Tube (PMT, Hamamatsu H10493-012:HA, 185–850 nm). Additionally, a miniature fiber optic spectrometer (Ocean Optics, QE65000, range 200–1100 nm) coupled with a 1000 μm diameter fiber optic (QP1000- 2-UV-VIS) was employed for TL and RL spectroscopy measurements. To assess the functionality of the system, it was used to measure TL and RL from Al_2O_3:C,Mg, Al_2O_3:C and TLD-100 phosphors which have been previously well investigated. The measured TL and RL data were well compared to the published ones, confirming the functionality of the system.

1. Introduction

Thermoluminescence (TL) and radioluminescence (RL) have been extensively used to evaluate materials for dosimetric applications. TL refers to the light emitted by certain materials (such as crystals or semiconductors) when heated, representing a thermally stimulated emission of energy previously stored in the material during irradiation (McKeever, 1985). This technique finds applications in various fields including personal, medical, space, retrospective, and environmental dosimetry (McKeever, 1985; E G Yukihara et al., 2022; Yukihara, 2022). Similarly, RL, also known as X-ray excited optical luminescence (XEOL), corresponds to the luminescence emitted by a material while exposed to ionizing radiation (França et al., 2019; Nunes et al., 2020; Pagonis et al., 2014). RL covers several phenomena, including scintillation, Cherenkov radiation, and phosphorescence induced by ionizing radiation (Klein et al., 2019). Scintillation occurs when luminescent material absorbs high-energy photons and then emits visible light (Greskovich and Duclos, 1997; Pan et al., 2020). Scintillators are employed in real-time dosimetry for applications such as medical diagnostics, industrial inspection, nuclear medicine, and high-energy physics.

RL provides insights into luminescent centers in materials, which can serve as recombination centers in the TL technique (Park et al., 2018). Meanwhile, TL signals offer information regarding both traps and the recombination centers (McKeever, 2022). Moreover, TL spectroscopy offers valuable insights into the nature of the luminescence centers, thereby complement RL in the advancement of new luminescent dosimeters. TL spectroscopy has proven effective in studying the thermal activation energy of shallow and deep traps (Islam et al., 2019).

Additionally, the capability to measure RL as a function of temperature enables the acquisition on information regarding the thermal quenching of the defect-based luminescence centers (Trindade and Jacobsohn, 2018). Consequently, TL, RL, and their variants, such as TL spectroscopy, are highly valuable and powerful techniques for investigating defects in solids within the field of radiation dosimetry. These diverse techniques and methodologies used in dosimetry require instrumentation capable of obtaining information with high accuracy, a development has been observed in both commercial and custom-made systems.

* Corresponding author
E-mail address: neilotrindade@usp.br (N.M. Trindade).

https://doi.org/10.1016/j.apradiso.2024.111516
Received 29 May 2024; Received in revised form 5 September 2024; Accepted 9 September 2024
Available online 10 September 2024
0969-8043/© 2024 Elsevier Ltd. All rights are reserved, including those for text and data mining, AI training, and similar technologies.

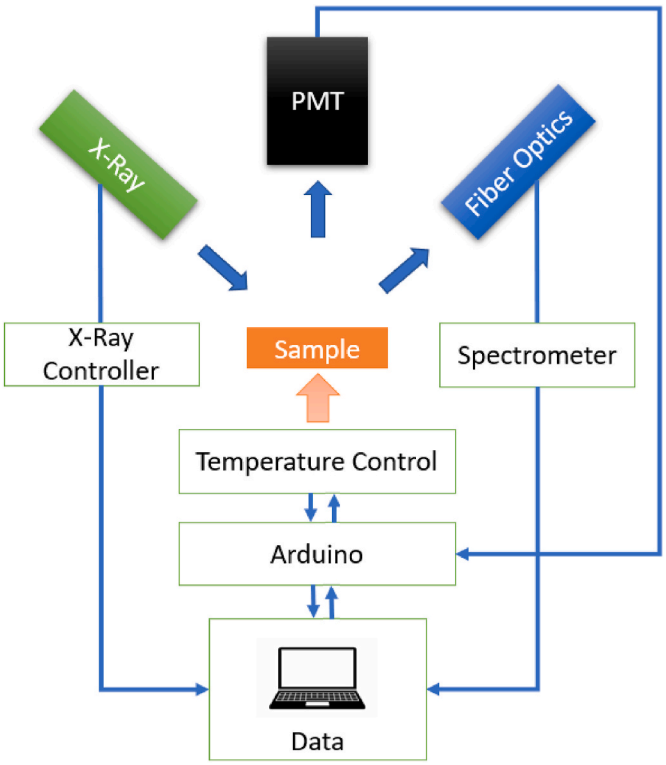

Fig. 1. Schematic layout of LUMI22. The optical fiber and the X-ray source are placed and inclined at 45° from the sample position.

In the early 1980s, the first automated TL reader, the Risø (model TL-DA-8), was introduced to the market (Bøtter-Jensen, 1998). This automated Risø reader quickly gained widespread adoption, being utilized in numerous laboratories to routinely conduct large volume of TL measurements with automatic sample changing capabilities (Bøtter-Jensen, 1998; Markey et al., 1997). Over the years, many researchers have been looking for ways to improve the commercial TL readers or develop their own readers with improved resolution and accuracy (Bøtter-Jensen, 1998; França et al., 2019; Markey et al., 1997). Luff and Townsend (1992) integrated a pair of spectrometers and photomultiplier tubes (PMTs) to create a high-sensitivity TL reader. They also enhanced photon counting sensitivity of the reader across the wavelength range from 200 to 800 nm. Rhodes et al. (2000) developed a high-resolution TL reader by incorporating a charge-coupled device (CCD) array into the spectrometer (Sony ILX511), achieving a photon counting sensitivity of 86 photons/count and extending the spectrum range from 200 to 1100 nm. Recently, the *LEXSYG* system developed by Freiberg Instruments company has emerged as a versatile commercial modular system capable of TL measurements a well as Optically Stimulated Luminescence (OSL), Infrared Stimulated Luminescence (IRSL), and fluorescence excited by ionizing radiation measurements (Richter et al., 2013).

Other researchers have proposed custom-made TL readers as alternatives to commercial ones, addressing the financial constraints associated with acquiring commercial systems. Tsuchiya et al. (2016) developed a portable, and desktop TL measurement system to facilitate in-situ measurements during geothermal field exploration. Park et al. (2018) introduced a custom-made system capable of performing various measuring tasks, including TL, OSL, and RL, either individually or simultaneously, with the ability to measure RL-OSL or RL-TL concurrently. Similarly, França et al. (2019) built a TL-RL system capable of working with both techniques.

The primary aim of our work was to develop a custom-made reader, specifically designed to facilitate simultaneous analysis. This system, named LUMI22, is compact, ensuring ease of use while also offering greater affordability compared to commercial alternatives. LUMI22 is capable of simultaneously or selectively measuring TL, RL, as well as performing TL and RL spectroscopy as functions of temperature. We provide detailed descriptions of the system's setup, heating rate, and control implementation, demonstrating its unique capabilities.

2. Instrumentation

The main parts of the TL-RL system include a heating system which can heat the sample to 400 °C at controlled heating rates; and a light collection system, which offers insights into the intensity and/or wavelength of light emitted by the sample. One other component incorporated is a data acquisition system for acquiring and processing luminescence signals. A mechanical structure was constructed to enclose these components, ensuring the radiological safety of users and maintain the electrical system's components safe from interference by radiation. Fig. 1 shows the system setup flowchart.

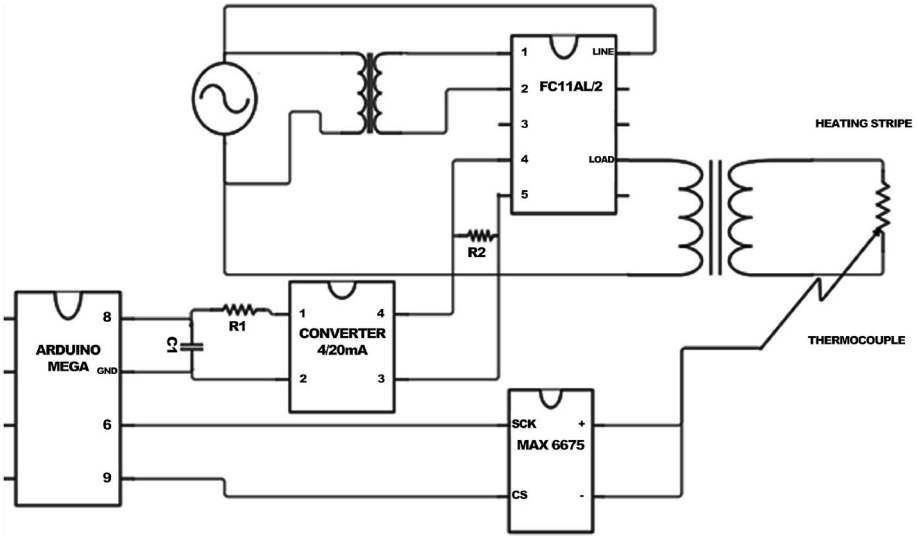

Fig. 2. Electronic diagram of the heating system.

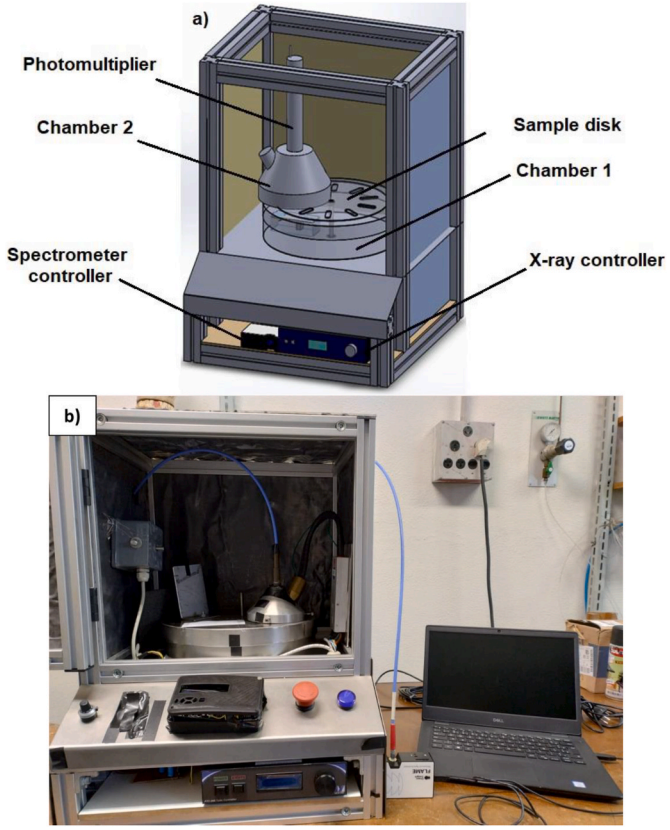

Fig. 3. a) Design in modeling software SolidWorks v2013: Chamber 1 is the place with the carousel and a part of the servo motor. Chamber 2 is the place where the measurements are performed, where the photomultiplier, the X-ray tube, and the spectrometer's optical fiber are allocated. b) Prototype assembled in the laboratory.

Table 1
Specifications of the LUMI22 system.

Analysis	Equipment	Characteristics/Setting
TL	Photomultiplier tube	Spectral response from 185 to 850 nm
RL	Spectrometer	Wavelength range from 200 to 1100 nm
RL	Optical fiber	Range detection from 300 to 1025 nm
RL	X-ray tube	40 kV/40 μA; dose rate 0.43 Gy/min

2.1. Heating system

The heating system used a universal phase angle controller (FC11AL/2 - United Automation Ltd) to regulate a low-voltage transformer. The high-power transformer supplied power to a resistor, heating the planchet constructed from an iron-chromium-aluminum alloy, within which the sample was positioned. For temperature monitoring, a K-type thermocouple was affixed under the kanthal plate (sample holder) and connected to an integrated circuit (model MAX6675), enabling temperature readings up to 1024 °C with a resolution of 0.25 °C. The thermocouple has an accuracy of 8 least significant bits (LSBs) for temperatures ranging from 0 to 700 °C. Further details can be seen in Fig. 2.

2.2. X-ray irradiation

The compact X-ray tube (Magnum 50 kV, 50 μA, TUB00050-W01 - *Moxtek Inc.*), featuring a tungsten target, served as the ionizing radiation source, delivering a high flux within a small area. The FTC-200 Source Controller powers, controls, and monitors X-ray source, allowing adjustment of high voltage and emission current. It provides input power to the high-voltage supply and displays real-time power settings for the X-ray tube.

2.3. Light detection system

A PMT Hamamatsu (H10493-012:HA) coupled to an Arduino model UNO was incorporated for integral light measurement. The system is fitted with an optical fiber (QP1000-2-UV/VIS) coupled at a spectrometer (QE65000), both from Ocean Optics, for TL and RL spectra collection. This system boasts a wavelength detection range from 300 to 1025 nm. Our system configuration used a fixed spectrometer arrangement with multi-measurements, enabling simultaneous detection across all wavelength channels. In this assembly, no filters were used.

2.4. Control system

The temperature and light signal control were implemented using the LabVIEW language integrated with the Arduino IDE platform. The output signal used for temperature control was in pulse width modulation (PWM) form, emitted by an Arduino port. This signal generated by the controller was converted into a default 4–20 mA signal and directly affected the phase angle controller de-vice on the low-voltage transformer, adjusting the current in the high-current transformer. The control loop was closed with the acquisition of temperature data by the K-type thermocouple. In the control system, the generated signals and received data are managed by the Arduino controller. The PID (Proportional, Integral, and Derivative) algorithm compares the difference between the set point and temperature read on the heating plate, generating a new PWM signal. This signal consequently controls the current in the high-voltage transformer, regulating the heating of the sample. Furthermore, the adjustment of PID gains was performed using the Ziegler-Nichols method (Ogata, 2005; Ziegler and Nichols, 1949).

2.5. Mechanical structure

A structural aluminum profile was designed using *SolidWorks* v2013 (Fig. 3a). The structure was constructed with dimensions of 46 × 46 × 60 cm^3 as shown in Fig. 3b. The system was segmented into two parts: the bottom part, housing the electronics; and the top part, accommodating the TL-RL measurement chamber.

The electronics components were shielded from ionizing radiation and temperature effects by the construction of a chamber of stainless steel, with a thickness of 3 mm, enabling the incorporation of the heating system. The entire system was shielded with a lead sheet, 0.5 mm thick, to ensure radiation protection. The multi-sample disk facilitated system automation without requiring operator intervention, thereby preventing interference during measurements.

2.6. Dose Rate calculation at the sample position

To evaluate the dose rate delivered to sample position, thermoluminescent dosimeters (TLDs) were used. A set of 16 LiF (Bycron, TLD-100) detectors were exposed to the radiation generated by the compact X-ray tube described in section 2.2. One group of 8 detectors was individually irradiated at the sample holder for 10s, while the other group was exposed for 20s. The tube potential of 40 kV/40 μA remained constant for all exposures. Four detectors from each group were positioned between a lead filter of (0.50 ± 0.05) mm thickness, while the remaining four detectors were exposed without any filter. This configuration facilitated the determination of the photon-effective energy incident on the detector.

For dose evaluation, a subset of detectors, previously selected based on TL response, were exposed to known kerma in air values from a ^{137}Cs source. An ionization chamber of 6 cm^3 (Radcal Co.), positioned at the same location (227 cm from the source) as the samples, was utilized to

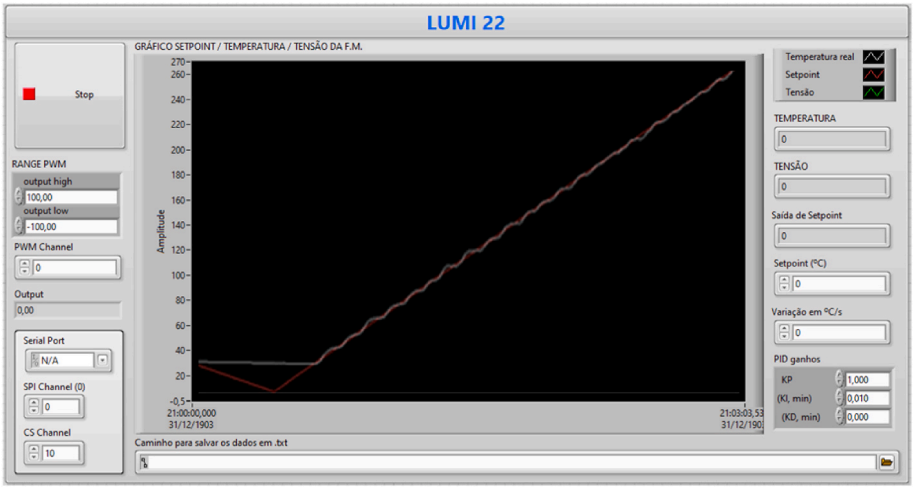

Fig. 4. Interface of software created based in LabVIEW showing a temperature ramp graphic. Set point (red line) and temperature in real-time (white line). (For interpretation of the references to colour in this figure legend, the reader is referred to the web version of this article.)

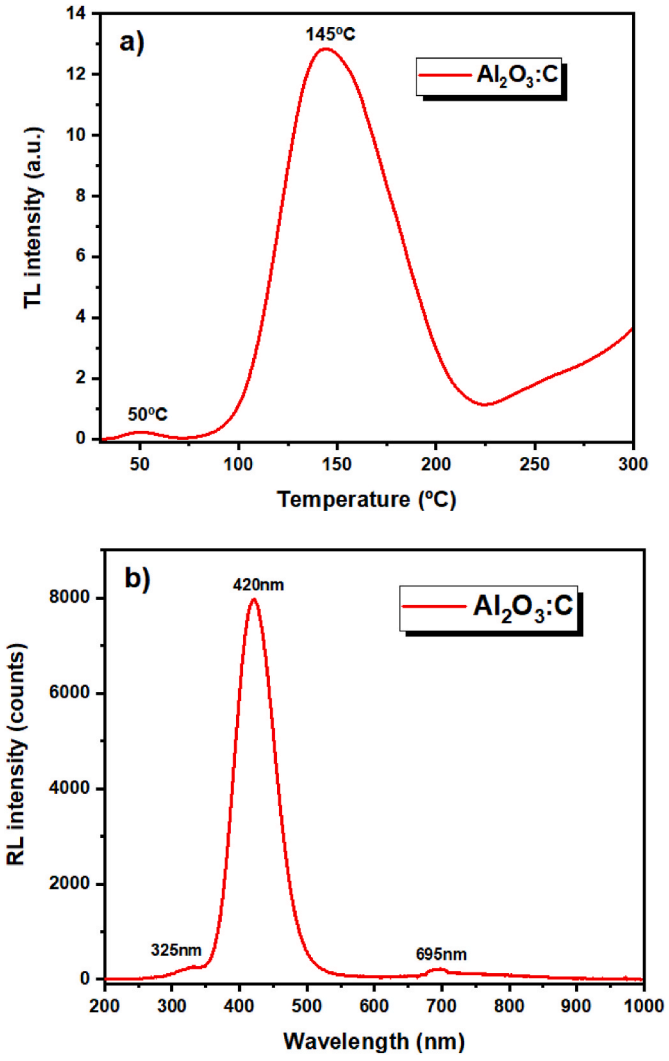

Fig. 5. a) TL glow curve of Al_2O_3:C. The sample was previously irradiated with 1 Gy from X-rays and heated at a rate of 3 °C/s. b) RL spectrum of Al_2O_3:C acquired with an integration rate of 60s.

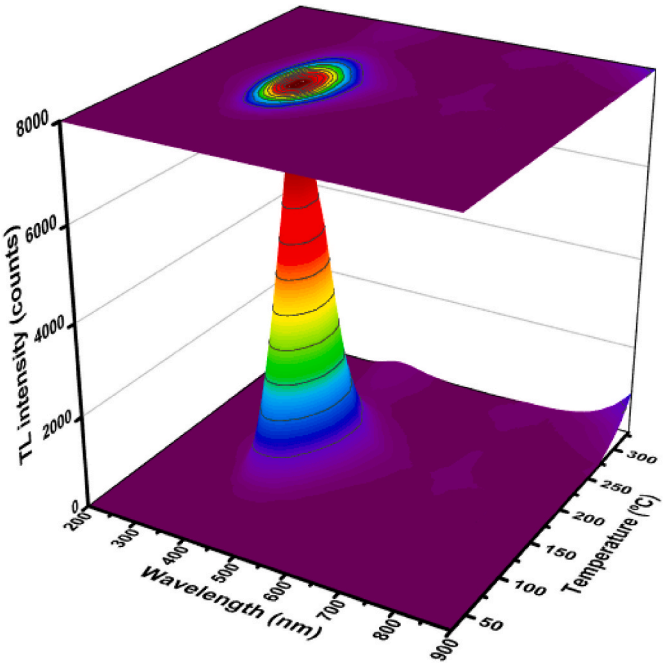

Fig. 6. TL spectrum of Al_2O_3:C exposed to 4.3 Gy from X-rays obtained in LUMI22 system.

measure the kerma in air values ranging from 1.6 mGy to 48 mGy. The slope of the linear relationship between TL intensity and kerma in air values provided the calibration factor necessary to determine dose equivalent values. The methodology for dose evaluation and photon energy determination is the same procedure applied in the individual monitoring service at the Laboratory of Dosimetry of the University of São Paulo (Okuno et al., 2017). An automated TL/OSL reader (Risø model DA-20) was used for TL readout with data analysis performed using QtiPlot software. Finally, a summary of all the specifications of the LUMI22 system is presented in Table 1.

3. Results and discussion

3.1. Temperature ramps

For accurate generation of thermoluminescence curves, precise

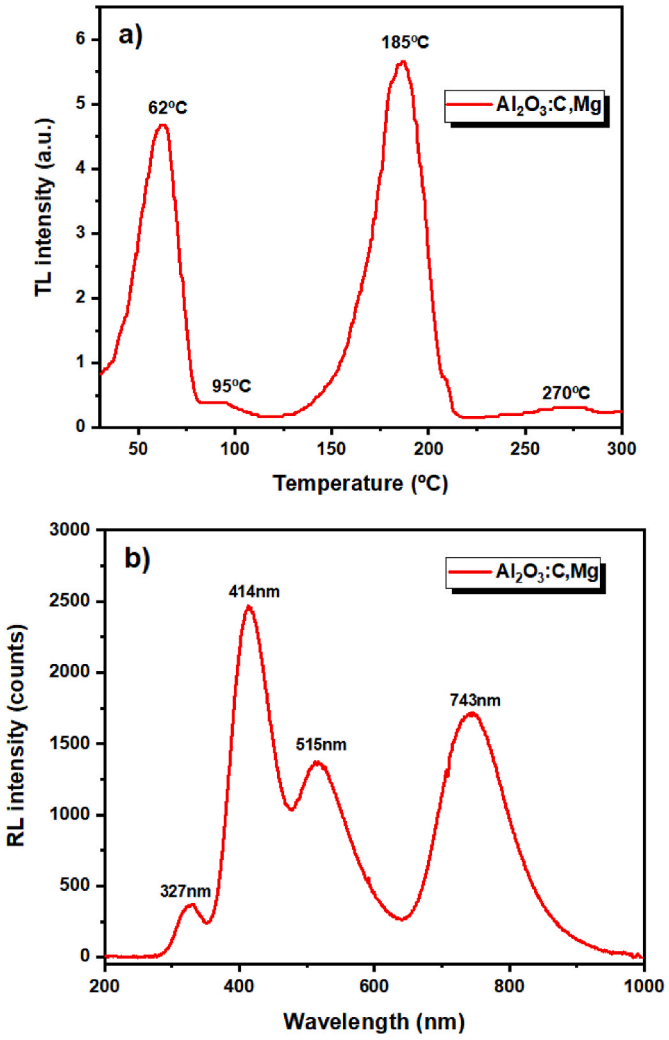

Fig. 7. a) TL glow curve of Al_2O_3:C,Mg. The sample was previously irradiated with 4.5 Gy from X-rays and heated at a rate of 1 °C/s. b) RL spectrum of Al_2O_3:C,Mg acquired with an integration rate of 60s.

adjustment of the control system and the heating ramps is essential, optimized by PID gains. The developed system enables the generation of curves with heating rates ranging from 1 to 5 °C/s, with the transformer output power regulated to accommodate common heating rates used in TL. The interface of the system is shown in Fig. 4.

Numerous tests were conducted to achieve optimal adjustment for heating rates between 1 and 5 °C/s. PID values were calculated and tested iteratively until the heating ramp closely matched the setpoint. Fig. 4 illustrates the program interface and provides an example of one of the PID adjustments made. To control the PID gains, it was necessary to restrict the PWM signal to 45 % due to the high-current intensity in the power-transformer.

3.2. Dose rate obtained at the sample position

The dose rate obtained at the sample position, as determined using TLDs, was measured to be 7.1 mGy/s. Based on the responses of detectors with and without filters, it can be inferred that the incident photon energy is lower than 30 keV when the fixed tube potential of 40 kV/40 μA is used. This calibration was chosen to ensure consistency and comparability in our measurements. The variation in dose rate settings (not shown here) was explored to understand its effect on the RL signal, and the results demonstrated that the 40 kV/40 μA setting provided the most reliable and intense response.

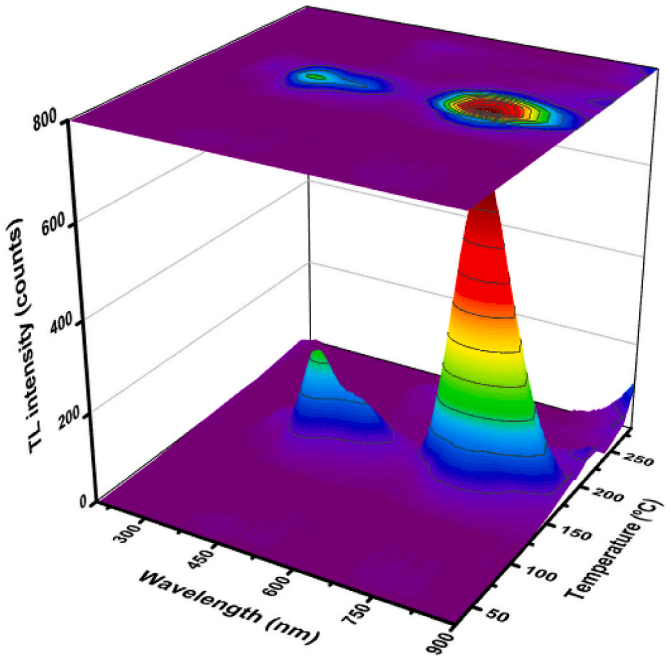

Fig. 8. TL spectrum of Al_2O_3:C,Mg exposed to 4.3 Gy from X-rays obtained in LUMI22 system.

3.3. TL and RL spectra of commercial dosimeters

Several tests were carried out to evaluate the LUMI-22 system, utilizing samples of Al_2O_3:C,Mg, Al_2O_3:C, and TLD-100. The Al_2O_3:C,Mg sample used in this study was grown by the Czochralski technique (Akselrod et al., 2003; Brandle, 2004), commercially produced by *LANDAUER Inc.* The sample was cut into a rectangular parallelepiped ($8.0 \times 1.6 \times 0.5$ mm^3) weighing 48 mg. Likewise, the Al_2O_3:C sample was produced by *LANDAUER Inc.*, but in this work, powder samples weighing 50 mg were used. The last sample used was TLD-100 (Bicron) with dimensions of ($3.2 \times 3.2 \times 1.0$ mm^3).

For thermoluminescent measurements, the samples were irradiated with ~1 Gy (40 kV/40 μA source) and then heated up to 300 °C. RL experiments were carried out from the sample at room temperature, with an integration time of 60 s. TL spectra were collected for the samples previously exposed to ~4.3 Gy. The samples were heated up to ~300 °C at a rate of 1 °C/s. For the acquisition of spectra, an integration time of 15s was chosen, meaning the spectra were saved every 15 °C.

3.3.1. Al_2O_3:C

Carbon-doped alumina (Al_2O_3:C) is widely studied in the field of dosimetry as a thermoluminescence dosimeter with high sensitivity (Akselrod et al., 1990). Al_2O_3:C has applications in personal and environmental dosimetry using ionizing radiation (Kalita and Chithambo, 2017; Yukihara and McKeever, 2006). The high sensitivity of this material is attributed to C doping in Al_2O_3, which promotes the formation of a large concentration of color centers, also known as F and F^+ (Kalita and Chithambo, 2017). In Fig. 5, the results for TL (with a heating rate of 3 °C/s) and RL signals of Al_2O_3:C are presented. Two glow peaks were observed, one centered at 50 °C and another at 145 °C. These emissions are consistent with findings in the literature, particularly regarding the dosimetric peak. Chithambo et al. (2014) performed TL measurements at 0.4 °C/s and reported the main glow peak of Al_2O_3:C at 156 °C, and two others at 36 and 268 °C. Ogundare et al. (2013) analyzed the TL response of this similar sample and identified the dosimetric glow peak around 200 °C, along with two smaller peaks at 74 and 342 °C with a heating rate of 5 °C/s. In the RL spectrum, three emissions were observed at 325, 420, and 695 nm, with the main emission occurring at

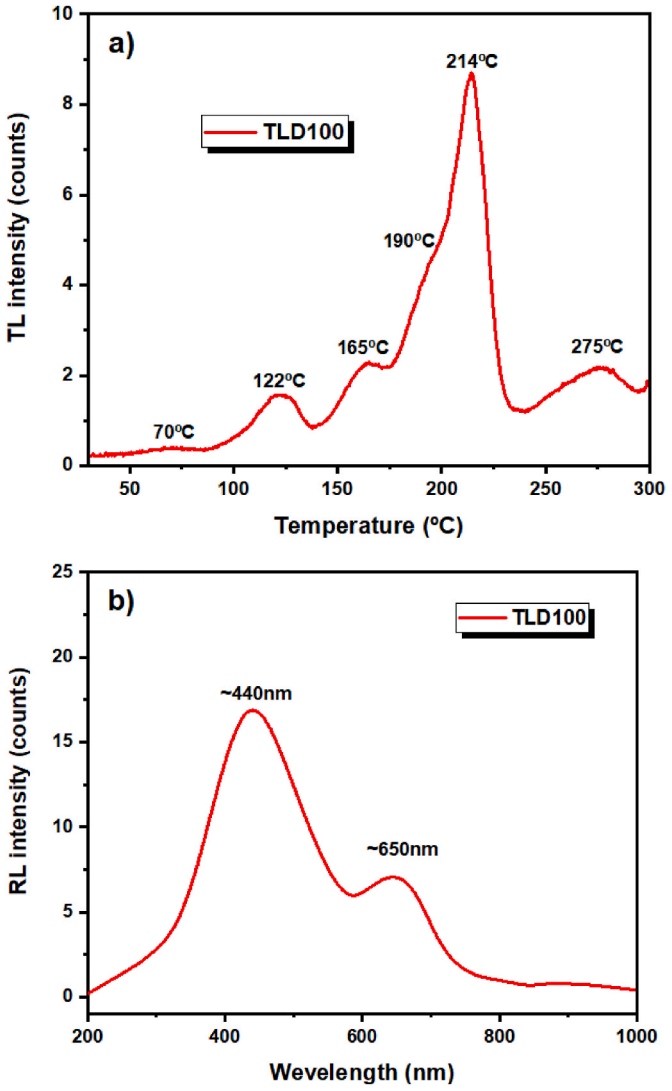

Fig. 9. a) TL glow curve of TLD-100. The sample was previously irradiated with 4.5 Gy from X-rays and heated at a rate of 1 °C/s. b) RL spectrum of TLD-100 acquired with an integration rate of 60 s.

420 nm. This emission pattern aligns with previous works in the literature. For example, Rodriguez et al. (2011) obtained RL results for Al_2O_3:C, reporting an intense peak at 415 nm and another peak with a low signal at 325 nm. These emissions are associated respectively to the F and F^+ centers.

Fig. 6 shows the TL spectrum of Al_2O_3:C. The sample exhibited two emissions peaks at 425, and 695 nm corresponding to the glow peak at 175 °C, with the emission at 425 nm being the most intense among those observed. Rodriguez et al. (2011) obtained similar results for this sample, reporting a large emission peak in the TL spectrum at 415 nm associated with the F centers.

3.3.2. Al_2O_3:C,Mg

Al_2O_3:C,Mg is widely studied as a dosimetric material and has demonstrated its applicability for a wide spectrum of radiations (Kalita and Chithambo, 2017; Kalita and Chithambo, 2018; Munoz et al., 2021; Rodriguez et al., 2011; Saharin et al., 2014; Trindade et al., 2020, 2019; Trindade and Jacobsohn, 2018), with a particular emphasis on neutron dosimetry (Akselrod and Sykora, 2011; Sykora et al., 2007, 2008). The increase in the concentration of F and F+centers, along with the formation of aggregated and perturbed F-type centers (F^+(Mg), F^{2+}(Mg), F^{2+}(Mg), F^+(2 Mg), F^{2+}(2 Mg), F^{2+}(2 Mg)), promotes an increase in

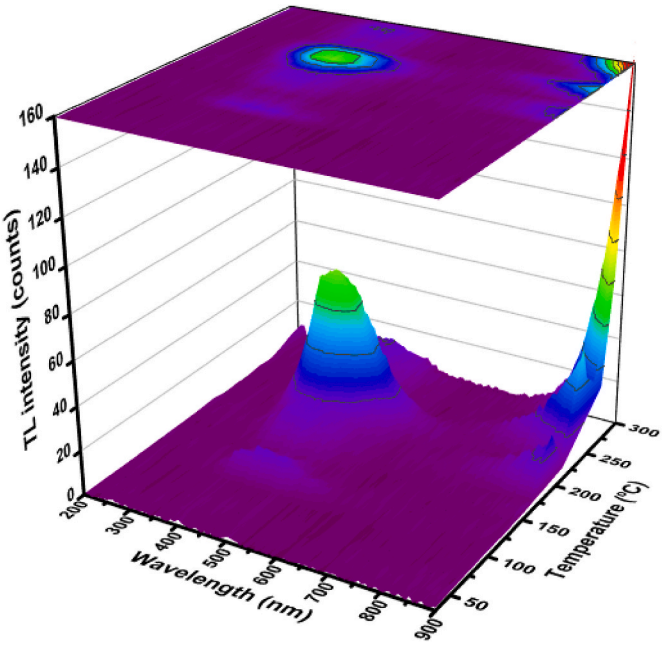

Fig. 10. TL spectrum of TLD100 exposed to 4.3 Gy from X-rays obtained in LUMI-22 system.

luminescence intensity (Chithambo et al., 2022).

Fig. 7 shows the TL (with a heating rate of 1 °C/s) and RL spectrum of Al_2O_3:C,Mg. Four glow peaks were observed, centered at ~60, ~95, ~185 and ~ 270 °C. Similarly, Chithambo et al. (2020) reported two glow peaks at 60 °C and 150 °C when the Al_2O_3:C,Mg was exposed to the X-ray irradiation dose of 3.6 Gy. In the RL spectrum, peaks were observed at ~330, ~415, ~515, and ~740 nm. According to Chithambo et al. (2020), RL measurements with a sample exposed to X-rays at room temperature (30 °C) exhibited two emission bands centered at 420 nm and 510 nm, which aligns with the results shown in Fig. 7b. Moreover, Peto and Kelemen (1996), using beta radiation, reported an emission band appearing between 410 and 420 nm that is associated with F center, being the most intense band in the radioluminescence from Al_2O_3:C and Al_2O_3:C,Mg. In addition, as noted by Akselrod and Kortov (1990) and Akselrod et al. (2003), the band about 325 nm is associated with F^+ centers, and Mg doping induces new broad RL bands at ~ 520 and ~ 750 nm, attributed $F^{(2+)}$(2 Mg), F^+ (2 Mg) centers, respectively.

Fig. 8 shows the TL spectrum of Al_2O_3:C,Mg. Four emissions were observed, centered at ~325, ~420, ~510, and ~740 nm, all with the highest emission temperature at 165 °C. Additionally, a lower intensity glow peak was notable at 250 °C with an emission centered at ~530 nm. This observation aligns with previous findings, suggesting that the glow peak centered at 165 °C may also be associated with the traps responsible for the glow peak at 185 °C. The TL spectrum correlates with the results of RL, sharing similar explanations as mentioned earlier. Furthermore, Chithambo et al. (2020) obtained results of TL spectra for unannealed and annealed samples of Al_2O_3:C,Mg. The unannealed sample showed two emission bands at 330 and 410 nm at a temperature of 150 °C, while the annealed sample showed bands at 330 nm and 410 nm at temperatures of 60 and 155 °C, respectively. These emission centers closely match those obtained in this work.

3.3.3. TLD-100

LiF:Mg,Ti, commercially known as TLD-100, is extensively employed in individual and area monitoring, as well as a luminescence dosimetry (Yukihara et al., 2022). LiF:Mg,Ti was initially synthesized by Morehead and Daniels in 1952, subsequently patented by the Harshaw Chemical Company in 1963 (Horowitz et al., 2019). It has been commercially available in three isotopic forms: TLD-100 (natural Li), used in this

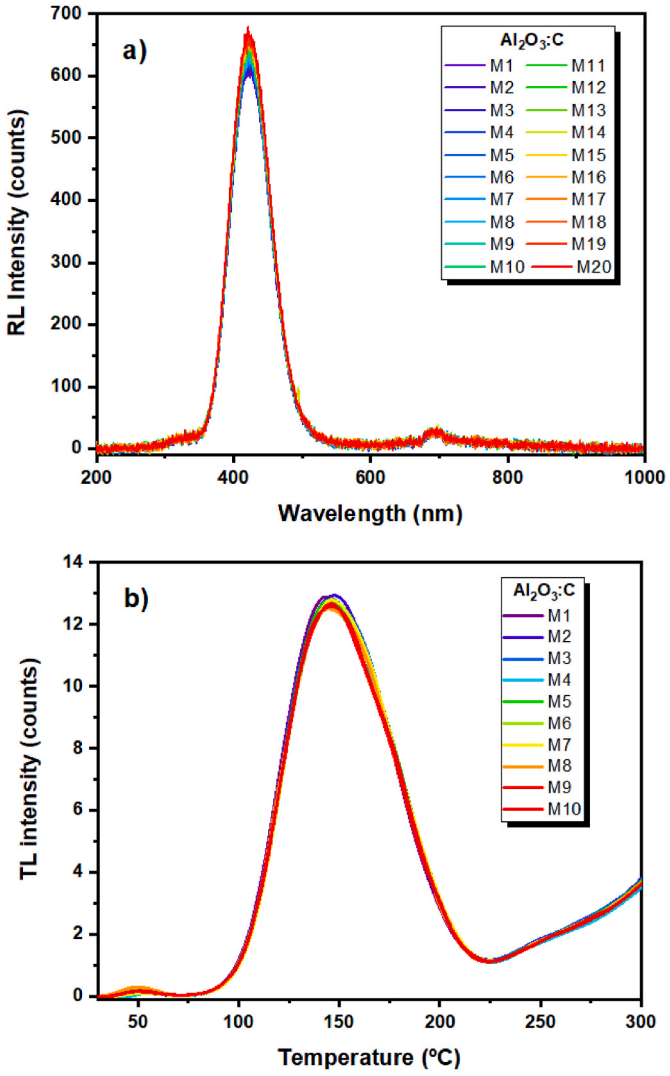

Fig. 11. Repeatability analysis of Al_2O_3:C. a) Radioluminescence with 20 measurement cycles with an integration time of 20 s. b) Thermoluminescence with 10 measurements performed at a dose of 1 Gy and heating rate of 3 °C/s.

study, and TLD-600 (enriched 6Li), and TLD-700 (enriched 7Li) (Horowitz et al., 2019).

Fig. 9 shows the TL (with a heating rate of 1 °C/s) and RL spectrum of TLD-100. The TL glow curve of TLD100 exhibited six glow peaks, with the main and most intense peak occurring around 215 °C. The shape of the curve and the observed peaks closely resemble those found in other studies (Horowitz et al., 2019; Yukihara et al., 2022). For example, Horowitz et al. (2019) reported the occurrence of the most intense glow peak at 200 °C, with a heating rate of 1 °C/s. The RL analysis revealed two emissions at ~440 and ~650 nm, with the most intense peak previously reported in the literature with emission around 410 nm (Pető and Kelemen, 1995; Zimmerman, 1971). Additionally, Pető and Kelemen (1995) identified other less intense peaks around 460, 520, and 560 nm, attributing these emissions to radiation-induced optical absorption bands present in the pure LiF matrix.

Fig. 10 shows the TL spectrum of TLD-100. The spectrum shows a large emission peak at ~430 nm, related with the maximum intensity observed at ~210 °C. This emission is also evident at temperatures of 120, 170, and 275 °C. In addition, for temperatures above 200 °C, notable emissions in the infrared region are observed, which have not yet been influenced by the black-body radiation emitted during the heating of the kanthal plate.

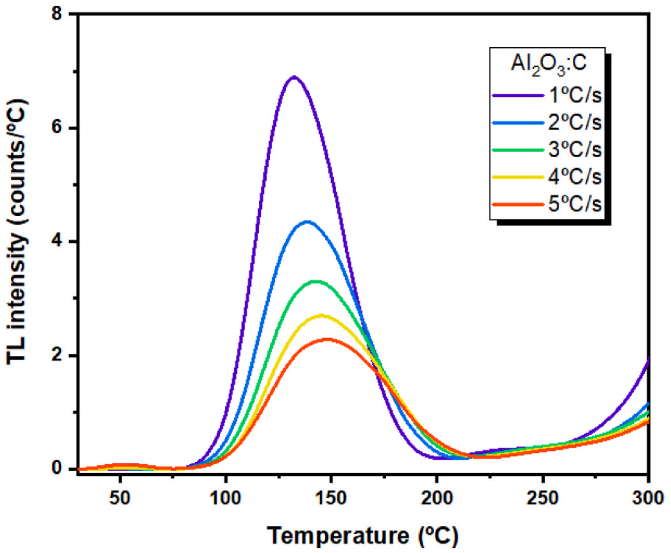

Fig. 12. TL glow curves of Al_2O_3:C previously irradiated with 1Gy, for different heating rates (from 1 up to 5 °C/s).

3.3.4. *Repeatability and various heating rates*

To evaluate the repeatability of the RL signal, 20 measurement cycles were performed using Al_2O_3:C sample with an integration time of 20 s. Repeatability tests were also conducted for the TL using the same Al_2O_3:C sample, with 10 measurements performed at a dose of 1 Gy and heating rate of 3 °C/s. The results are shown in Fig. 11.

For RL measurements, we focused on the main peak, where the sample exhibited a coefficient of variation (CV) of 2.6 %. The RL peak also presented the following characteristics: a full width at half maximum (FWHM) of 68.9 ± 0.5, a peak intensity of (648 ± 17) counts, and a peak position of (422 ± 2) nm. For TL measurements, the main glow peak showed a CV of 1.3 %, with a FWHM of 64.5 ± 0.5, a peak intensity of 12.7 ± 0.2 counts, and peak position of (146.0 ± 0.9) °C. These results underscore the high reliability of the measurements obtained with the LUMI22 system.

In addition, we also performed TL measurements with heating rate variation tests ranging from 1 up to 5 °C/s using the Al_2O_3:C sample, with the results summarized in Fig. 12. An increase in glow peak intensities was observed, as well as the shift in the temperatures associated with the main glow peak as the heating rate varied. This behavior is consistent with observations in other materials (Chithambo et al., 2014; Yazici et al., 2003). The results indicate that the heating curves in the TL measurements using LUMI22 are suitable, allowing the use of heating rates from 1 to 5 °C without affecting the measurement parameters (such as PID or transformer power control).

4. Conclusion

In this study, an integrated thermoluminescence-radioluminescence measurement system has been developed, denoted as LUMI22. The system demonstrated excellent performance in generating temperature ramps, achieving temperatures ranging from room temperature up to ~350 °C with different heating rates (1 up to 5 °C/s). The software implemented to perform measurements and temperature control proved to be effective for laboratory tests and small-scale sampling.

The estimated dose rate at the sample position on LUMI22 was ~0.43 Gy/min. The tests conducted with Al_2O_3:C,Mg, Al_2O_3:C, and TLD100 yielded results consistent with those reported in the literature, confirming the reliability of the custom-made system. Furthermore, the results of the repeatability and heating rate variation tests using the Al_2O_3:C sample further attest to the robustness of the LUMI22 system. The low coefficients of variation observed in both RL and TL

measurements highlight the system's consistent and reliable performance. Moreover, the total cost of developing the prototype equipment, including materials and labor costs but excluding software e licenses, was estimated to be approximately US$ 40,000.00. This cost-effective solution demonstrates that the LUMI22 system meets the expectations for experimental techniques such TL, RL, TL spectroscopy, and RL as a function of temperature in the field of ionizing radiation dosimetry. Overall, the system offers a cost-efficient alternative compared to commercial systems while maintaining high-quality performance.

CRediT authorship contribution statement

Matheus C.S. Nunes: Writing – review & editing, Writing – original draft, Methodology, Investigation, Formal analysis, Data curation. **Miguel L. Rodrigues:** Writing – original draft, Software, Methodology, Data curation, Conceptualization. **Walace J.R. Silva:** Writing – review & editing, Writing – original draft, Methodology, Formal analysis, Data curation. **Ronaldo S. Silva:** Writing – original draft, Validation, Supervision, Methodology, Formal analysis, Conceptualization. **Nancy K. Umisedo:** Writing – original draft, Methodology, Data curation. **Elisabeth M. Yoshimura:** Writing – original draft, Validation, Resources, Funding acquisition. **Neilo M. Trindade:** Writing – review & editing, Writing – original draft, Resources, Project administration, Methodology, Funding acquisition, Conceptualization.

Declaration of competing interest

The authors declare that they have no known competing financial interests or personal relationships that could have appeared to influence the work reported in this paper.

Data availability

Data will be made available on request.

Acknowledgments

N. M. Trindade is grateful to FAPESP (#2018/05982–0; #2019/05915–3) and CNPq (#409338/2021–4). W. J. R. Silva is grateful to FAPESP (#2021/00626-3) and CAPES. M. C. S. Nunes is grateful to FAPESP (#2021/12758-1; #2022/14516-8). R. S. Silva is grateful to FAPESP (#2021/08653-0). E. M. Yoshimura is grateful to FAPESP (#2018/05982–0) and CNPq (#311657/2021–4). The authors would like to thank Prof. Dr. Alexandre Brincalepe Campo and B.Sc. Brayan Oliveira da Silva, both from Federal Institute of São Paulo, for the support given in the development of the first version of the control system. The authors also express their gratitude to the students F. R. Kobata, J. V. V. Faria and F. S. Costa for their assistance in the ongoing maintenance of the equipment.

References

Akselrod, M.S., Akselrod, A.E., Orlov, S.S., Sanyal, S., Underwood, T.H., 2003. New aluminum oxide single crystals for volumetric optical data storage. In: Optical Data Storage. Optical Society of America, Vancouver, p. TuC3. https://doi.org/10.1364/ODS.2003.TuC3.

Akselrod, M.S., Kortov, V.S., 1990. Thermoluminescent and exoemission properties of new high-sensitivity TLD $α$ - $Al_2O_3:C$ crystals. Radiat. Protect. Dosim. 33, 123–126.

Akselrod, M.S., Kortov, V.S., Kravetsky, D.J., Gotlib, V.I., 1990. Highly sensitive thermoluminescent anion-defective α-Al_2O_3:C single crystal detectors. Radiat. Protect. Dosim. 32, 15–20. https://doi.org/10.1093/oxfordjournals.rpd.a080771.

Akselrod, M.S., Sykora, G.J., 2011. Fluorescent nuclear track detector technology – a new way to do passive solid state dosimetry. Radiat. Meas. 46, 1671–1679. https://doi.org/10.1016/j.radmeas.2011.06.018.

Bøtter-Jensen, L., 1998. Luminescence techniques: instrumentation. Radiat. Meas. 27, 749–768.

Brandle, C.D., 2004. Czochralski growth of oxides. J. Cryst. Growth 264, 593–604.

Chithambo, M.L., Kalita, J.M., Finch, A.A., 2020. F- and F^+-band radioluminescence and the influence of annealing on its emission spectra in Al_2O_3:C,Mg. Radiat. Meas. 134, 106306 https://doi.org/10.1016/j.radmeas.2020.106306.

Chithambo, M.L., Kalita, J.M., Trindade, N.M., 2022. Processes related to phototransfer under blue- and green-light illumination in annealed Al 2 O 3 :C,Mg. J. Appl. Phys. 131, 245101 https://doi.org/10.1063/5.0094547.

Chithambo, M.L., Seneza, C., Ogundare, F.O., 2014. Kinetic analysis of high temperature secondary thermoluminescence glow peaks in α-Al2O3:C. Radiat. Meas. 66, 21–30. https://doi.org/10.1016/j.radmeas.2014.04.025.

França, L.V.S., Oliveira, L.C., Baffa, O., 2019. Development of a thermoluminescence and radioluminescence integrated spectrometer. Measurement 134, 492–499. https://doi.org/10.1016/j.measurement.2018.10.101.

Greskovich, C., Duclos, S., 1997. Ceramic scintillators. Annu. Rev. Mater. Sci. 27, 69–88.

Horowitz, Y.S., Oster, L., Eliyahu, I., 2019. The saga of the thermoluminescence (TL) mechanisms and dosimetric characteristics of LiF:Mg,Ti (TLD-100). J. Lumin. 214 https://doi.org/10.1016/j.jlumin.2019.116527.

Islam, M.M., Rana, D., Hernandez, A., Haseman, M., Selim, F.A., 2019. Study of trap levels in β-Ga 2 O 3 by thermoluminescence spectroscopy. J. Appl. Phys. 125, 055701 https://doi.org/10.1063/1.5066424.

Kalita, J.M., Chithambo, M.L., 2018. The effect of annealing and beta irradiation on thermoluminescence spectra of α-Al_2O_3:C,Mg. J. Lumin. 196, 195–200. https://doi.org/10.1016/j.jlumin.2017.12.036.

Kalita, J.M., Chithambo, M.L., 2017. On the sensitivity of thermally and optically stimulated luminescence of α-Al_2O_3:C and α-Al_2O_3:C,Mg. Radiat. Meas. 99, 18–24. https://doi.org/10.1016/j.radmeas.2017.03.006.

Klein, J.S., Sun, C., Pratx, G., 2019. Radioluminescence in biomedicine: physics, applications, and models. Phys. Med. Biol. 64, 04TR01 https://doi.org/10.1088/1361-6560/AAF4DE.

Luff, B.J., Townsend, P.D., 1992. High sensitivity thermoluminescence spectrometer. Meas. Sci. Technol. 3, 65–71.

Markey, B.O., Bøtter-Jensen, L., Duller, G.A.T., 1997. A new flexible system for measuring thermally and optically stimulated luminescence. Radiat. Meas. 27, 83–89.

McKeever, S.W.S., 2022. A Course in Luminescence Measurements and Analyses for Radiation Dosimetry. John Wiley & Sons, Chichester.

McKeever, S.W.S., 1985. Thermoluminescence of solids. Cambridge Solid State Science Series. Cambridge University Press, Cambridge. https://doi.org/10.1017/cbo9780511564994.

Munoz, J.M., Lima, L.S., Yoshimura, E.M., Jacobsohn, L.G., Trindade, N.M., 2021. OSL response of α-Al2O3:C, Mg exposed to beta and UVC radiation: a comparative investigation. J. Lumin. 236, 118058 https://doi.org/10.1016/j.jlumin.2021.118058.

Nunes, M.C.S., Lima, L.S., Yoshimura, E.M., França, L.V.S., Baffa, O., Jacobsohn, L.G., Malthez, A.L.M.C., Kunzel, R., Trindade, N.M., 2020. Characterization of the optically stimulated luminescence (OSL) response of beta-irradiated alexandrite-polymer composites. J. Lumin. 226, 6–11. https://doi.org/10.1016/j.jlumin.2020.117479.

Ogata, K., 2005. Engenharia de Controle Moderno, fourth ed. Pearson.

Ogundare, F.O., Ogundele, S.A., Chithambo, M.L., Fasasi, M.K., 2013. Thermoluminescence characteristics of the main glow peak in α-Al2O3:C exposed to low environmental-like radiation doses. J. Lumin. 139, 143–148. https://doi.org/10.1016/j.jlumin.2013.02.034.

Okuno, E., Umisedo, N.K., Cancio, F.S., Aldred, M.A., Yoshimura, E.M., 2017. Three decades of occupational individual monitoring at the University of São Paulo. Radiat. Protect. Dosim. 177, 285–288. https://doi.org/10.1093/rpd/ncx042.

Pagonis, V., Chithambo, M.L., Chen, R., Chruścińska, A., Fasoli, M., Li, S.H., Martini, M., Ramseyer, K., 2014. Thermal dependence of luminescence lifetimes and radioluminescence in quartz. J. Lumin. 145, 38–48. https://doi.org/10.1016/j.jlumin.2013.07.022.

Pan, L., Daguano, J.K.M.F., Trindade, N.M., Cerruti, M., Zanotto, E.D., Jacobsohn, L.G., 2020. Scintillation, luminescence and optical properties of Ce-Doped borosilicate glasses. Opt. Mater. (Amst). 104, 109847 https://doi.org/10.1016/j.optmat.2020.109847.

Park, C.Y., Park, Y.K., Chung, K.S., Lee, J.D., Kim, J.L., 2018. An Integrated System for radioluminescence, thermoluminescence and optically stimulated luminescence measurements. J. Radiat. Prot. Res. 43, 160–169.

Peto, A., Kelemen, A., 1996. Radioluminescence properties of alpha $AL2O3$ TL dosemeters. Radiat. Prot. Dosim. OSA Tech. Dig. Ser. 65, 139–142.

Pető, Á., Kelemen, A., 1995. Radioluminescence of LiF:Mg,Ti induced by 4 MeV electrons. Radiat. Meas. 24, 571–573. https://doi.org/10.1016/1350-4487(95)00166-C.

Rhodes, M.W., Wanwilairat, S., Vilaithong, T., Hoffmann, W., 2000. Low cost high resolution thermoluminescence spectrometer. Rev. Sci. Instrum. 71, 2053–2057. https://doi.org/10.1063/1.1150577.

Richter, D., Richter, A., Dornich, K., 2013. Lexsyg - a new system for luminescence research. Geochronometria 40, 220–228.

Rodriguez, M.G., Denis, G., Akselrod, M.S., Underwood, T.H., Yukihara, E.G., 2011. Thermoluminescence, optically stimulated luminescence and radioluminescence properties of Al_2O_3:C,Mg. Radiat. Meas. 46, 1469–1473. https://doi.org/10.1016/j.radmeas.2011.04.026.

Saharin, N.S., Wagiran, H., Tamuri, A.R., 2014. Thermoluminescence (TL) properties of Al2O3: C, Mg exposed to cobalt-60 gamma radiation doses. Radiat. Meas. 70, 11–14. https://doi.org/10.1016/j.radmeas.2014.08.012.

Sykora, G.J., Akselrod, M.S., Salasky, M., Marino, S.A., 2007. Novel Al_2O_3:C,Mg fluorescent nuclear track detectors for passive neutron dosimetry. Radiat. Protect. Dosim. 126, 278–283. https://doi.org/10.1093/rpd/ncm058.

Sykora, G.J., Salasky, M., Akselrod, M.S., 2008. Properties of novel fluorescent nuclear track detectors for use in passive neutron dosimetry. Radiat. Meas. 43, 1017–1023. https://doi.org/10.1016/j.radmeas.2007.12.038.

Trindade, N.M., Jacobsohn, L.G., 2018. Thermoluminescence and radioluminescence of α-Al2O3:C,Mg at high temperatures. J. Lumin. 204, 598–602. https://doi.org/10.1016/j.jlumin.2018.08.018.

Trindade, N.M., Jacobsohn, L.G., Yoshimura, E.M., 2019. Correlation between thermoluminescence and optically stimulated luminescence of α-Al2O3:C,Mg. J. Lumin. 206, 298–301. https://doi.org/10.1016/j.jlumin.2018.10.084.

Trindade, N.M., Magalhães, M.G., Nunes, M.C.S., Yoshimura, E.M., Jacobsohn, L.G., 2020. Thermoluminescence of UV-irradiated α-Al2O3:C,Mg. J. Lumin. 223, 117195 https://doi.org/10.1016/j.jlumin.2020.117195.

Tsuchiya, N., Ishikawa, H., Saito, R., Hirano, N., 2016. Development of portable thermoluminescence measurement equipment for geothermal exploration. J. Geotherm. Res. Soc. Japan 38, 127–131.

Yazici, A.N., Solak, S., zt rk, Z., Topaksu, M., Yegingil, Z., 2003. The analysis of dosimetric thermoluminescent glow peak of -Al 2 O 3 : C after different dose levels by -irradiation. J. Phys. D Appl. Phys. 36, 181–191. https://doi.org/10.1088/0022-3727/36/2/318.

Yukihara, E.G., 2022. TL and OSL as research tools in luminescence: possibilities and limitations. Ceram. Int. https://doi.org/10.1016/j.ceramint.2022.10.199.

Yukihara, E.G., Bos, A.J.J., McKeever, S.W.S., 2022. The quest for new thermoluminescence and optically stimulated luminescence materials : needs , strategies and pitfalls. Radiat. Meas. 158.

Yukihara, E.G., McKeever, S.W.S., 2006. Spectroscopy and optically stimulated luminescence of Al_2O_3: C using time-resolved measurements. J. Appl. Phys. 100 https://doi.org/10.1063/1.2357344.

Yukihara, Eduardo G., McKeever, S.W.S., Andersen, C.E., Bos, A.J.J., Bailiff, I.K., Yoshimura, E.M., Sawakuchi, G.O., Bossin, L., Christensen, J.B., 2022. Luminescence dosimetry. Nat. Rev. Methods Prim. 21 (2), 1–21. https://doi.org/10.1038/s43586-022-00102-0, 2022.

Ziegler, J.G., Nichols, N.B., 1949. Dynamic accuracy in temperature measurement. Science 110, 361–363. https://doi.org/10.1126/science.110.2858.361.

Zimmerman, J., 1971. The radiation-induced increase of thermoluminescence sensitivity of the dosimetry phosphor LiF(TLD-100). J. Phys. C Solid State Phys. 4, 3277–3291. https://doi.org/10.1088/0022-3719/4/18/033.